Observation of math xmlns="http://www.w3.org/1998/Math/MathML" display="inline">mn>1/mn>mo>//mo>msup>mi>k/mi>mn>4/mn>/msup>/math>-Tails after Expansion of Bose-Einstein Condensates with Impurities

Hugo Cayla, Pietro Massignan, Thierry Giamarchi, Alain Aspect, Christoph I. Westbrook, and David Clément

Phys. Rev. Lett. **130**, 153401 — Published 12 April 2023

DOI: 10.1103/PhysRevLett.130.153401

Observation of $1/k^4$-tails after expansion of Bose-Einstein Condensates with impurities

Hugo Cayla,[1] Pietro Massignan,[2] Thierry Giamarchi,[3] Alain Aspect,[1] Christoph I. Westbrook,[1] and David Clément[1]

[1] *Université Paris-Saclay, Institut d'Optique Graduate School, CNRS, Laboratoire Charles Fabry, 91127, Palaiseau, France*

[2] *Departament de Física, Universitat Politècnica de Catalunya, Campus Nord B4-B5, E-08034 Barcelona, Spain*

[3] *Department of Quantum Matter Physics, University of Geneva, 24 quai Ernest-Ansermet, 1211 Geneva, Switzerland*

(Dated: March 6, 2023)

We measure the momentum density in a Bose-Einstein condensate (BEC) with dilute spin impurities after an expansion in the presence of interactions. We observe tails decaying as $1/k^4$ at large momentum k in the condensate and in the impurity cloud. These algebraic tails originate from the impurity-BEC interaction, but their amplitudes greatly exceed those expected from two-body contact interactions at equilibrium in the trap. Furthermore, in the absence of impurities, such algebraic tails are not found in the BEC density measured after the interaction-driven expansion. These results highlight the key role played by impurities when present, a possibility that had not been considered in our previous work [Phys. Rev. Lett. **117**, 235303 (2016)]. Our measurements suggest that these unexpected algebraic tails originate from the non-trivial dynamics of the expansion in the presence of impurity-bath interactions.

Impurities strongly affect the properties of low-temperature ensembles of particles. Well-known examples range from the Kondo effect [1–4], to quantum localization [5–7] and polar crystals [8, 9]. Similarly, the transport of massive impurities strongly depends on the medium in which they propagate and scatter, as illustrated in experiments conducted with gaseous Bose-Einstein condensates (BECs) as a bath [10–16]. Impurities can also serve as accurate probes for equilibrium and out-of-equilbrium properties of their many-body environment [17–21].

Theoretical approaches introduce a quasi-particle, the polaron, which describes the dressing of the impurity by the collective excitations of the bath [22, 23]. In quantum gas experiments, such descriptions were validated in ensembles of both bosons and fermions [24–26]. Furthermore, the capability to tune interactions in atomic gases permitted detailed studies beyond the weakly-interacting regime [27–30]. However, recent theoretical work [31–33] illustrated the need for a precise knowledge of the impurity-bath interaction to accurately describe Bose polarons and quantities such as their energy in the strongly-interacting regime. Tan's contact provides direct information on short-ranged interaction potentials in systems at equilibrium [34] and it was measured recently for Bose polarons [29]. Here, we investigate an out-of-equilibrium configuration and observe unexpected signals resulting from the impurity-BEC interaction.

In our experiments we measure momentum densities after an expansion of dilute BECs containing weakly-interacting impurities. We observe that: *(i)* the momentum densities of the impurities and of the BEC exhibits algebraic tails whose decay is consistent with $1/k^4$ over a surprisingly large momentum range, *(ii)* the algebraic tails are observed only in the presence of both the BEC and the impurities, and *(iii)* the tail amplitude increases linearly with the number of impurities. These features qualitatively resemble those expected from two-body interactions at equilibrium in the trap. However, the tail amplitude is orders of magnitudes larger than the expected in-trap impurity contact. Our observation is even more surprising, because the in-trap $1/k^4$-tails associated with the impurity-BEC contact are expected to vanish adiabatically during the expansion in the presence of interactions [35]. This suggests that the expansion dynamics of the impurity-bath system plays a key role here. Interestingly, $1/k^4$-tails of amplitude larger than those expected in the trap were similarly observed in a SU(N) Fermi gas [36]. These could result from inter-component interactions present during the expansion [36], the analog of the impurity-bath interaction in our case.

We also revisit our previous observation of $1/k^4$-tails in an expanding BEC [37]. Our earlier experiment was conducted under conditions identical to the present ones. Dilute impurities were very likely present there as well, but we were not aware of their presence. Here we show unambiguously that the tails disappear when the impurities are removed from the BEC, and we confirm the scenario predicted theoretically [35]. This conclusion differs from that of recent work [38] where similar $1/k^4$-tails were found in expanding BECs without impurities.

In our experiment the bath is a BEC of metastable Helium-4 (^{4}He*) atoms in the $m_J = +1$ sub-level and the impurities are a small number of ^{4}He* atoms in the $m_J = 0$ sub-level. The impurity-bath scattering length $a_{IB} \simeq 142\ a_0$ is equal to the scattering length within the BEC, $a_{BB} \simeq 142\ a_0$ [39], with a_0 the Bohr radius. Our experiment starts with the production of a degenerate Bose gas of ^{4}He* atoms in a crossed optical dipole trap (ODT) [40]. The evaporation to BEC is performed with (most of) the atoms polarised in the $m_J = +1$ magnetic sub-level to avoid the inelastic collisions present in non-

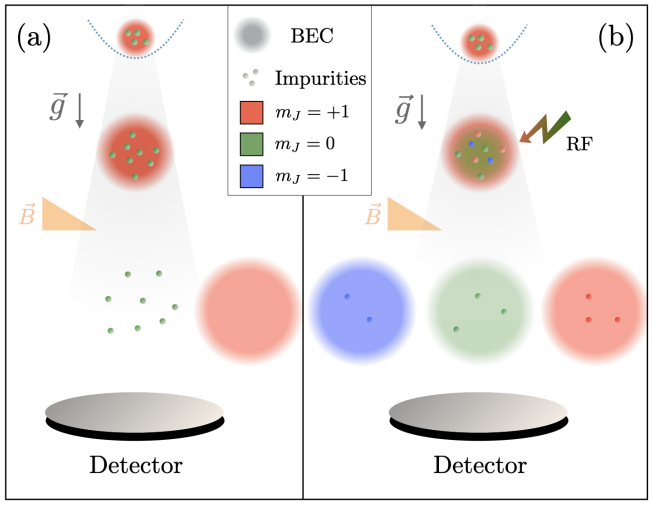

FIG. 1. **(a)** To detect only spin impurities ($m_J = 0$), a magnetic gradient is applied during the expansion to push the BEC atoms ($m_J = +1$) away from the detector. **(b)** To probe simultaneously BEC atoms and impurities, a radio-frequency (RF) pulse couples the atomic states $m_J = 0$ and $m_J = +1$ during the expansion, before applying the magnetic gradient, producing a known mixture of $m_J = 0$ and $m_J = \pm 1$.

polarised ^{4}He* gases [41]. The final ODT frequencies are $\omega_x/2\pi = 110$ Hz, $\omega_y/2\pi = 400$ Hz and $\omega_z/2\pi = 420$ Hz. The polarisation of the atoms is maintained in the ODT with a magnetic bias field of ~ 4 G, but this does not ensure a full spin-polarisation of the gas. Indeed, we recently discovered that a small fraction ($f_I \lesssim 1\%$) of spin impurities ($m_J = 0$ atoms) is present. These impurities originate from spin flips occurring during the loading of the ODT from a magnetic quadrupole trap [40]. This previously unnoticed situation is an opportunity to study Bose polarons in a flat-bottom potential. Indeed, given that a_{BB} and a_{IB} are equal, the mean-field interaction of impurities with the BEC exactly cancels the harmonic trapping potential confining them [42].

In the following, we concentrate on the tails of the momentum density at large momenta, exploiting our ability to record extremely small densities [43]. Our investigation builds upon *(i)* tuning the number of impurities N_I and the BEC atom number $N_{\rm BEC}$ independently, and *(ii)* detecting selectively the spin sub-levels. We vary $N_{\rm BEC}$ from 1×10^4 to 1×10^6 by modifying the shape of the optical trap [44]. The impurity fraction f_I is varied between 0.05% and 1% using optical pumping and varying holding times in the trap [44]. Once we have prepared the trapped gas, we switch off the trap and let the gas expand in free-fall for a long time-of-flight (TOF) $t_{\rm TOF} = 298$ ms. Exploiting the different magnetic properties of $m_J = +1$ and $m_J = 0$ atoms, we selectively detect the two spin sub-levels. More precisely, we can choose to detect only atoms initially trapped in the $m_J = 0$ state by pulsing a magnetic gradient during the expansion to push the $m_J = +1$ atoms away from the detector (see Fig. 1a). Alternatively, we can detect a known fraction of both initially trapped $m_J = +1$ and $m_J = 0$ atoms (see Fig. 1b). After 10 μs of expansion and before applying the magnetic gradient, we shine a radio-frequency pulse (of duration 30 μs) to transfer a known fraction of $m_J = +1$ atoms into the $m_J = 0$ state.

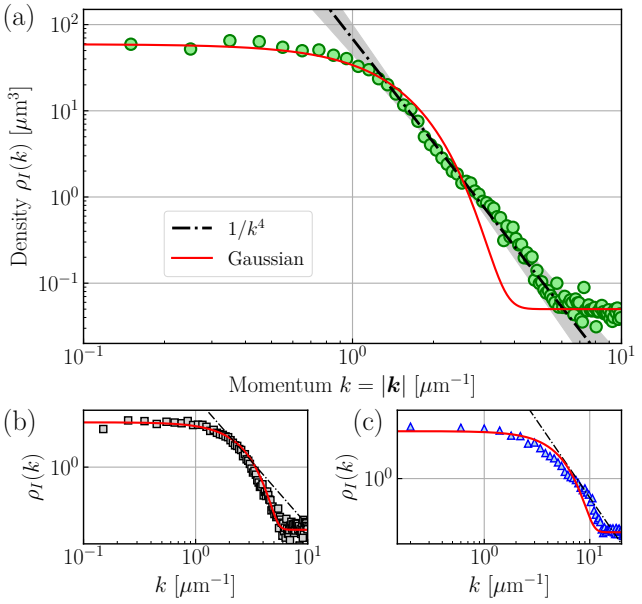

FIG. 2. **(a)** Momentum density $\rho_{\rm I}(k)$ of impurities in a spin-polarised BEC (green dots). The dashed-dotted black line is an algebraic decay $\propto 1/k^4$ and the grey shaded corresponds to power-law functions $1/k^\alpha$ with $3.5 \leq \alpha \leq 4.5$. The red line is a fit with a Gaussian function. **(b)** $\rho_{\rm I}(k)$ in the absence of $m_J = +1$ atoms in the trap (black squares). The red dashed line is the Gaussian-shape density for an ideal Bose gas at $T \simeq 200$ nK. **(c)** $\rho_{\rm I}(k)$ in the presence of a thermal gas of $m_J = +1$ atoms in the trap (blue triangles). No algebraic decay is clearly identifiable.

In a first set of experiments, we measure the far-field momentum density $\rho_{\rm I}(\boldsymbol{k})$ of the spin impurities, normalized so that $\int d^3\boldsymbol{k}\ \rho_{\rm I}(\boldsymbol{k}) = N_I$. The momentum $\boldsymbol{k}$ of an atom is determined from the measured 3D position $\boldsymbol{r}$ after TOF using the ballistic relation, $\boldsymbol{k} = m\boldsymbol{r}/\hbar t_{\rm TOF}$. Recall that the density $\rho_{\rm I}(\boldsymbol{k})$ measured after a long expansion differs from the in-trap momentum density as interactions affect the early stages of the expansion. Importantly, in all the data sets presented in this work, $\rho_{\rm I}(\boldsymbol{k})$ is found isotropic. This allows us to increase the signal-to-noise ratio in $\rho_{\rm I}$ by taking a spherical average and study $\rho_{\rm I}$ as a function of the modulus $k = |\boldsymbol{k}|$, as shown in Fig. 2. The dataset in Fig. 2(a) is recorded with $N_{\rm BEC} = 4.4(3) \times 10^5$, and a fraction of impurities $f_{\rm I} \simeq 0.3(1)$ %. The density $\rho_{\rm I}(k)$ exhibits algebraic tails whose decay is consistent with $1/k^4$. Note that the observed decay does not span a large enough dynamical range to precisely determine the power-law exponent (see

[38] and Fig. 4). Figs. 2(b)-(c) show the same quantity measured in the absence of the BEC, in two different configurations. The density $\rho_{\rm I}$ shown in Fig. 2(b) is recorded in the absence of $m_J = +1$ atoms, so that only the impurity cloud is present in the trap, and it is well fitted by a Gaussian modelling a thermal gas. In Fig. 2(c), $\rho_{\rm I}$ is measured in the presence of a thermal gas of $m_J = +1$ atoms. In both Figs. 2(b)-(c) no algebraic decays are identified [45]. Algebraic tails are unambiguously observed in $\rho_{\rm I}$ only in the presence of a BEC.

In a second set of experiments, we measure the far-field momentum density of a cloud in which a known fraction of the trapped $m_J = +1$ BEC atoms is transferred to the detector (see Fig. 1b). We repeat the experiment and analysis performed in [37], but here we reduce the fraction of impurities to our smallest possible value $f_{\rm I} \simeq 0.05$ %. For a direct comparison with [37], we introduce the quantity $\mathcal{C} = (2\pi)^3\mathcal{A}$ from the the measured amplitude $\mathcal{A} = k^4 \times \rho(k)$ of the tails (fitted over the momentum range $2\mu{\rm m}^{-1} - 6\mu{\rm m}^{-1}$). In Fig. 3 we plot $\mathcal{C}$ divided by $N_{\rm BEC}$. We stress that $\mathcal{C}$ is extracted after an expansion in the presence of interactions. Therefore, $\mathcal{C}$ differs from Tan's contact at equilibrium in the trap.

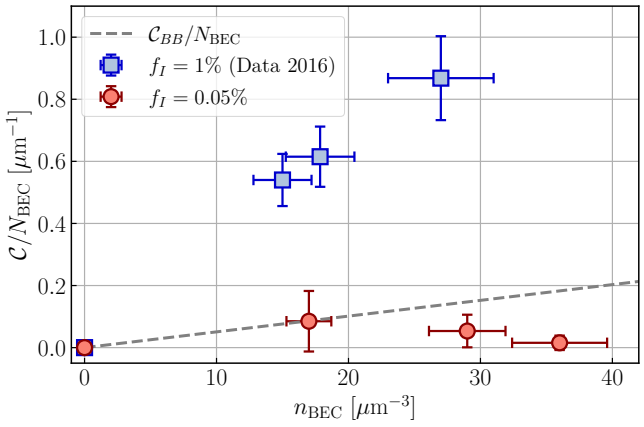

FIG. 3. Amplitude $\mathcal{C}$ of the $1/k^4$-tails in the BEC (normalised to $N_{\rm BEC}$) as a function of the BEC density, for two fractions of impurities $f_{\rm I} \sim 1$ % (blue squares - data from [37]) and $f_{\rm I} = 0.05$ % (red dots). The fraction $f_{\rm I} \sim 1$ % for the 2016 data is estimated by comparison with the new datasets (see Fig. 6a). The dashed-line is the in-trap contact $\mathcal{C}^{BB}_{\rm Bogo}/N_{\rm BEC}$ of a spin-polarised BEC [see Eq. (1)].

The values $\mathcal{C}/N_{\rm BEC}$ measured with $f_{\rm I} = 0.05\%$ lie much lower than those we found previously [37] and are consistent with zero (see Fig. 3). This uncovers the role played by the impurities in the findings we previously reported in [37]. In particular, this rules out the hypothesis that the tails are a direct signature of the quantum depletion of the spin-polarised BEC. Indeed, the resulting fitted amplitudes are much smaller than Tan's contact $\mathcal{C}^{BB}_{\rm Bogo}$ associated to the quantum depletion of a trapped spin-polarised BEC [37],

$$\mathcal{C}^{BB}_{\rm Bogo} = (64/7)\pi^2 a_{BB}^2 n_{\rm BEC} N_{\rm BEC}, \qquad (1)$$

where $n_{\rm BEC}$ indicates the BEC density at the trap center. Eq. (1) is obtained starting from Tan's contact for a homogeneous BEC, $C_0 = 16\pi^2 a_{BB}^2 n_{\rm BEC} N_{\rm BEC}$, and using a local density approximation (LDA) in the trap [37]. The LDA is safely applicable since $\xi \simeq 0.4\ \mu{\rm m} \ll R_z \simeq 15\ \mu{\rm m}$, where ξ is the BEC healing length and R_z the smallest in-trap BEC radius. Our observations confirm the scenario predicted theoretically in [35], i.e., that the $1/k^4$-tails associated with the quantum depletion of a spin-polarised BEC decrease adiabatically during an expansion in the presence of interactions. This conclusion differs from that of a recent work [38] which studied magnetically-trapped ^{4}He* atoms. So far, unambiguous signals of the quantum depletion in TOF experiments have been found only when interactions do not affect the expansion [46, 47].

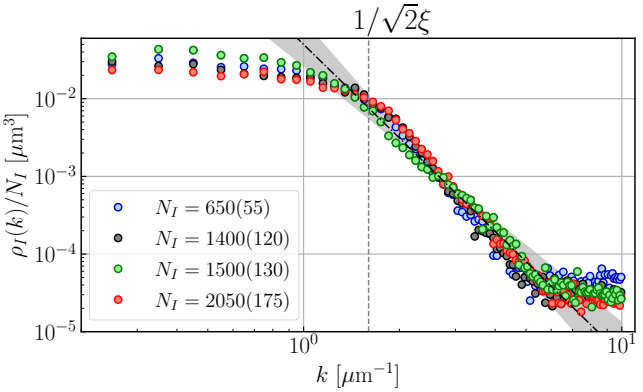

FIG. 4. Normalised density $\rho_I(k)/N_I$ as a function of k. The data sets correspond to a varying impurity number N_I in a BEC with a fixed number $N_{\rm BEC} = 4.5(5) \times 10^5$. The vertical dotted line indicates the momentum $k_{\rm c,BEC} = 1/\sqrt{2}\xi$ of the sound velocity in the BEC. The dashed-dotted line (*resp.* the grey shaded area) is a power-law function $1/k^\alpha$ with $\alpha = 4$ (*resp.* $3.5 \leq \alpha \leq 4.5$).

We turn to discussing the algebraic tails observed in the presence of both the BEC and impurities. To extract the tail amplitude $\mathcal{A}_{\rm BEC}$ (*resp.* $\mathcal{A}_I$) in the bath (*resp.* the impurity cloud), we combine the analysis of the data recorded with the two detection methods shown in Fig. 1 [48]. In a given data set, the tail amplitude $\mathcal{A}$ is obtained from fitting the plateau in $k^4 \times \rho(k)$ over the range $2\mu{\rm m}^{-1} - 6\mu{\rm m}^{-1}$. We have studied how $\mathcal{A}_{\rm BEC}$ and $\mathcal{A}_I$ change as we vary $N_{\rm BEC}$ and $N_{\rm I}$. A series of such measurements in the impurity cloud is shown in Fig. 4 where N_I is varied at fixed $N_{\rm BEC}$. The analysis of all the data sets is summarised in Figs. 5 and 6 [49].

In Fig. 5(a), we show that the amplitude $\mathcal{A}_I$ in the impurity cloud increases approximatively linearly with the number of impurities N_I. In Fig. 5(b), we observe that $\mathcal{A}_I$ also increases with the BEC density $n_{\rm BEC}$ at fixed N_I.

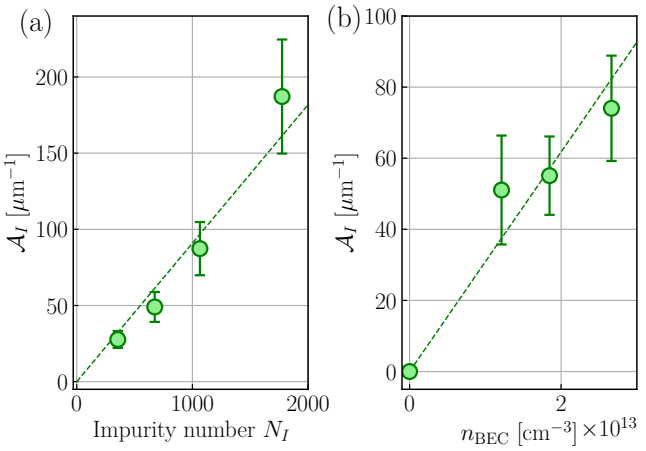

FIG. 5. **(a)** Amplitude $\mathcal{A}_{\rm I}$ of the $1/k^4$-tails in the impurity cloud as a function of N_I with a fixed to $N_{\rm BEC} = 5.5{\times}10^5$. **(b)** Amplitude $\mathcal{A}_{\rm I}$ as a function of $n_{\rm BEC}$ with a fixed $N_I = 770$. The point at $n_{\rm BEC} = 0$ corresponds to the data shown in Fig. 2(b). In both panels, the green dashed line is a guide-to-the-eye.

In Fig. 6(a), the amplitude $\mathcal{A}_{\rm BEC}$ in the majority (BEC) atoms is plotted as a function of N_I. Its growth is consistent with a linear increase with N_I. Interestingly, $\mathcal{A}_{\rm BEC}$ rapidly varies with $n_{\rm BEC}$ at fixed N_I [see Fig. 6(b)], with a scaling $\propto n_{\rm BEC}^{7/2}$ similar to that of the bath-bath contact $\mathcal{C}^{BB}_{\rm Bogo}$. We shall now discuss the possible origin of the algebraic tails.

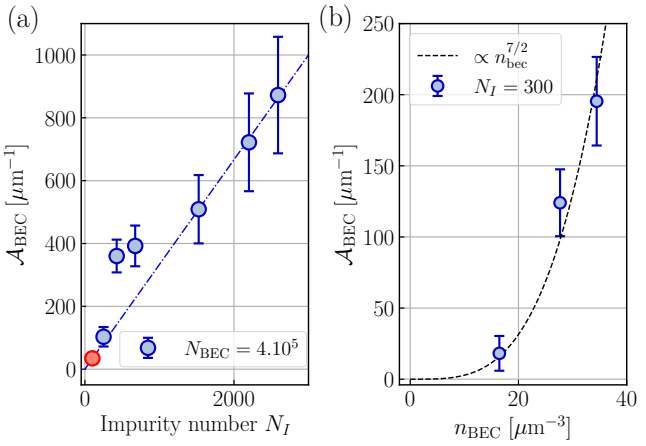

FIG. 6. **(a)** Amplitude $\mathcal{A}_{\rm BEC}$ of the $1/k^4$-tails in the BEC as a function of N_I. The red dot corresponds to the data set with $f_I \simeq 0.05\%$ shown in Fig. 3. The blue dashed line is a guide-to-the-eye. **(b)** Amplitude $\mathcal{A}_{\rm BEC}$ as a function of the BEC density $n_{\rm BEC}$ with $N_I = 300$. The dashed black line is proportional to $n_{\rm BEC}^{7/2}$.

In the regime of weak interactions investigated in the experiment, the *in-trap* momentum densities are known to have $1/k^4$-tails whose amplitudes are accurately described by Tan's contact. In the majority (BEC) atoms, Tan's contact results from the sum of two contributions: *(i)* the bath-bath interactions and *(ii)* the bath-impurity interactions. The bath-bath contact $\mathcal{C}^{BB}_{\rm Bogo}$ of Eq. (1) was derived in the LDA. Under similar assumptions, the bath-impurity contacts becomes $\mathcal{C}^{BI}_{\rm Bogo} = (32/5)\pi^2 a_{BI}^2 n_{\rm BEC} N_I$ [50]. In the impurity cloud, the interaction between impurities is negligible due to their small concentration, and only $\mathcal{C}^{BI}_{\rm Bogo}$ plays a significant role. However, as discussed above for a BEC without impurities, these $1/k^4$ signatures of two-body contact interactions are expected to vanish during the time-of-flight expansion in the presence of interactions [51]. This scenario does not match with our observations as the measured tails' amplitudes *largely exceed* the in-trap predictions. Therefore, our findings indicate that the algebraic tails result from the impurity-BEC interactions, but also that these are not a direct manifestation of two-body interactions at equilibrium. We speculate that they result from the expansion dynamics.

To complete our description, additional intriguing observations should be mentioned. First, the tail amplitude in the BEC is comparable to that in the impurity cloud ($\mathcal{A}_{\rm BEC} \sim 2-3\times\mathcal{A}_I$) while the BEC atom number exceeds that of impurities by several orders of magnitude ($N_I \lesssim N_{\rm BEC}/100$). This suggests that some equilibration between the momentum components of the impurities and of the BEC occurs during the expansion. Second, Fig. 4 shows that the algebraic tails are visible for momenta larger than $k_{c,\rm BEC} = 1/\sqrt{2}\xi$, the momentum associated with the BEC sound velocity $c = \sqrt{g_{BB} n_{\rm BEC}/m}$. Impurities moving faster than the BEC sound velocity – *i.e.*, the critical velocity for superfluidity – are known to create excitations in the BEC [52], contrary to slow moving impurities [53]. However, we performed GP simulations of the expansion dynamics of a BEC and a single impurity and we did not find $1/k^4$-tails in the momentum densities. Whether such effects play a role in our observations is an intriguing open question.

In conclusion, we have shown the crucial role of weakly-interacting spin impurities immersed in a Bose-Einstein condensate during an expansion in the presence of interactions and studied it quantitatively. The algebraic tails observed only in the presence of both the BEC and the impurities are not related to the in-trap contact, i.e., to short-range two-body physics at equilibrium, but rather result from the dynamics of moving impurities in an expanding superfluid bath. A detailed analysis of the complete expansion dynamics seems therefore crucial to understand our puzzling observations.

Acknowledgements. We acknowledge fruitful discussions with C. Carcy, M. Mancini, L. P. Pitaevskii, S. Stringari and all the members of the Quantum Gas group at Institut d'Optique, as well as technical help on the

apparatus from G. Hercé. We acknowledge financial support from the Région Ile-de-France in the framework of the DIM SIRTEQ, the "Fondation d'entreprise iX-core pour la Recherche", the Agence Nationale pour la Recherche (Grant number ANR-17-CE30-0020-01). D.C. acknowledges support from the Institut Universitaire de France. A.A. acknowledges support from the Simons Foundation (Grant 601939) and from Nokia-Bell labs. P.M. was supported by grant PID2020-113565GB-C21 funded by MCIN/AEI/10.13039/501100011033, by EU FEDER Quantumcat, by the National Science Foundation under Grant No. NSF PHY-1748958, and by the *ICREA Academia* program. This work was supported in part by the Swiss National Science Foundation under grant 200020-188687.

[1] Goldhaber-Gordon, D., Shtrikman, H., Mahalu, D., Abusch-Magder, D., Meirav, U. and Kastner, M. A., *Kondo effect in a single-electron transistor*, Nature **391**, 156 (1998).

[2] Cronenwett, S. M., Oosterkamp, T. H. and Kouwenhoven, L. P., *A Tunable Kondo Effect in Quantum Dots*, Science **281**, 540 (1998).

[3] Liang, W., Shores, M. P., Bockrath, M., Long, J. R. and Park, H., *Kondo resonance in a single-molecule transistor*, Nature **417**, 725 (2002).

[4] Alloul, H., Bobroff, J., Gabay, M. and Hirschfeld, P. J., *Defects in correlated metals and superconductors*, Rev. Mod. Phys. **81**, 45 (2009).

[5] Balatsky, A. V., Vekhter, I. and Zhu, J.-X., *Impurity-induced states in conventional and unconventional superconductors*, Rev. Mod. Phys. **78**, 373 (2006).

[6] Peres, N. M. R., *Colloquium: The transport properties of graphene: An introduction*, Rev. Mod. Phys. **82**, 2673 (2010).

[7] Ospelkaus, S., Ospelkaus, C., Wille, O., Succo, M., Ernst, P., Sengstock, K. and Bongs, K., *Localization of Bosonic Atoms by Fermionic Impurities in a Three-Dimensional Optical Lattice*, Phys. Rev. Lett. **96**, 180403 (2006).

[8] Fröhlich, H., *Electrons in lattice fields*, Advances in Physics **3**, 325 (1954).

[9] Feynman, R. P., *Slow Electrons in a Polar Crystal*, Phys. Rev. **97**, 660 (1955).

[10] Chikkatur, A. P., Görlitz, A., Stamper-Kurn, D. M., Inouye, S., Gupta, S. and Ketterle, W., *Suppression and Enhancement of Impurity Scattering in a Bose-Einstein Condensate*, Phys. Rev. Lett. **85**, 483 (2000).

[11] Palzer, S., Zipkes, C., Sias, C. and Köhl, M., *Quantum Transport through a Tonks-Girardeau Gas*, Phys. Rev. Lett. **103**, 150601 (2009).

[12] Zipkes, C., Palzer, S., Sias, C. and Köhl, M., *A trapped single ion inside a Bose–Einstein condensate*, Nature **464**, 388 (2010).

[13] Schmid, S., Härter, A. and Denschlag, J. H., *Dynamics of a Cold Trapped Ion in a Bose-Einstein Condensate*, Phys. Rev. Lett. **105**, 133202 (2010).

[14] Catani, J., Lamporesi, G., Naik, D., Gring, M., Inguscio, M., Minardi, F., Kantian, A. and Giamarchi, T., *Quantum dynamics of impurities in a one-dimensional Bose gas*, Phys. Rev. A **85**, 023623 (2012).

[15] Fukuhara, T. *et al.*, *Quantum dynamics of a mobile spin impurity*, Nature Physics **9**, 235 (2013).

[16] Balewski, J. B., Krupp, A. T., Gaj, A., Peter, D., Büchler, H. P., Löw, R., Hofferberth, S. and Pfau, T., *Coupling a single electron to a Bose–Einstein condensate*, Nature **502**, 664 (2013).

[17] Daley, A. J., Fedichev, P. O. and Zoller, P., *Single-atom cooling by superfluid immersion: A nondestructive method for qubits*, Phys. Rev. A **69**, 022306 (2004).

[18] Klein, A. and Fleischhauer, M., *Interaction of impurity atoms in Bose-Einstein condensates*, Phys. Rev. A **71**, 033605 (2005).

[19] Ng, H. T. and Bose, S., *Single-atom-aided probe of the decoherence of a Bose-Einstein condensate*, Phys. Rev. A **78**, 023610 (2008).

[20] Hohmann, M., Kindermann, F., Gänger, B., Lausch, T., Mayer, D., Schmidt, F. and Widera, A., *Neutral impurities in a Bose-Einstein condensate for simulation of the Fröhlich-polaron*, EPJ Quantum Technology **2**, 23 (2015).

[21] Skou, M. G., Skov, T. G., Jørgensen, N. B., Nielsen, K. K., Camacho-Guardian, A., Pohl, T., Bruun, G. M. and Arlt, J. J., *Non-equilibrium quantum dynamics and formation of the Bose polaron*, Nature Physics **17**, 731 (2021).

[22] Landau, L. D., *Uber die Bewegung der Elektronen in Kristalgitter*, Phys. Z. Sowjetunion **3**, 644 (1933).

[23] Pekar, S. I., *Autolocalization of the electron in an inertially polarizable dielectric medium*, Zh. Eksp. Teor. Fiz. **16**, 335 (1946).

[24] Devreese, J. T. and Alexandrov, A. S., *Fröhlich polaron and bipolaron: recent developments*, Reports on Progress in Physics **72**, 066501 (2009).

[25] Massignan, P., Zaccanti, M. and Bruun, G. M., *Polarons, dressed molecules and itinerant ferromagnetism in ultracold Fermi gases*, Reports on Progress in Physics **77**, 034401 (2014).

[26] Scazza, F., Zaccanti, M., Massignan, P., Parish, M. M. and Levinsen, J., *Repulsive Fermi and Bose Polarons in Quantum Gases*, Atoms **10**, 55 (2022).

[27] Jørgensen, N. B., Wacker, L., Skalmstang, K. T., Parish, M. M., Levinsen, J., Christensen, R. S., Bruun, G. M. and Arlt, J. J., *Observation of Attractive and Repulsive Polarons in a Bose-Einstein Condensate*, Phys. Rev. Lett. **117**, 055302 (2016).

[28] Hu, M.-G., Van de Graaff, M. J., Kedar, D., Corson, J. P., Cornell, E. A. and Jin, D. S., *Bose Polarons in the Strongly Interacting Regime*, Phys. Rev. Lett. **117**, 055301 (2016).

[29] Yan, Z. Z., Ni, Y., Robens, C. and Zwierlein, M. W., *Bose polarons near quantum criticality*, Science **368**, 190 (2020).

[30] Devreese, J. T., *Fröhlich Polarons. Lecture course including detailed theoretical derivations – 10th edition* (2020), arXiv:1611.06122 [cond-mat.other].

[31] Massignan, P., Yegovtsev, N. and Gurarie, V., *Universal Aspects of a Strongly Interacting Impurity in a Dilute Bose Condensate*, Phys. Rev. Lett. **126**, 123403 (2021).

[32] Schmidt, R. and Enss, T., *Self-stabilized Bose polarons*, SciPost Phys. **13**, 054 (2022).

[33] Levinsen, J., Ardila, L. A. P. n., Yoshida, S. M. and Parish, M. M., *Quantum Behavior of a Heavy Impurity Strongly Coupled to a Bose Gas*, Phys. Rev. Lett. **127**,

033401 (2021).
[34] Tan, S., *Large momentum part of a strongly correlated Fermi gas*, Annals of Physics **323**, 2971 (2008).
[35] Qu, C., Pitaevskii, L. P. and Stringari, S., *Expansion of harmonically trapped interacting particles and time dependence of the contact*, Phys. Rev. A **94**, 063635 (2016).
[36] Song, B., Yan, Y., He, C., Ren, Z., Zhou, Q. and Jo, G.-B., *Evidence for Bosonization in a Three-Dimensional Gas of* SU(N) *Fermions*, Phys. Rev. X **10**, 041053 (2020).
[37] Chang, R., Bouton, Q., Cayla, H., Qu, C., Aspect, A., Westbrook, C. I. and Clément, D., *Momentum-Resolved Observation of Thermal and Quantum Depletion in a Bose Gas*, Phys. Rev. Lett. **117**, 235303 (2016).
[38] Ross, J. A., Deuar, P., Shin, D. K., Thomas, K. F., Henson, B. M., Hodgman, S. S. and Truscott, A. G., *On the survival of the quantum depletion of a condensate after release from a magnetic trap*, Scientific Reports **12**, 13178 (2022).
[39] Leo, P. J., Venturi, V., Whittingham, I. B. and Babb, J. F., *Ultracold collisions of metastable helium atoms*, Phys. Rev. A **64**, 042710 (2001).
[40] Bouton, Q., Chang, R., Hoendervanger, A. L., Nogrette, F., Aspect, A., Westbrook, C. I. and Clément, D., *Fast production of Bose-Einstein condensates of metastable helium*, Phys. Rev. A **91**, 061402 (2015).
[41] Shlyapnikov, G. V., Walraven, J., Rahmanov, U. M. and Reynolds, M. W., *Decay Kinetics and Bose Condensation in a Gas of Spin-Polarized Triplet Helium*, Phys. Rev. Lett. **73**, 3247 (1994).
[42] Note that spin impurities in the $m_J = -1$ magnetic sublevel, if present after the optical trap loading, are rapidly lost in the presence of a BEC and expected to play no role in our observations. These rapid losses are due to the large rate of Penning collisions between $m_J = -1$ and $m_J = +1$ atoms, which exceeds by four orders of magnitude that between $m_J = 0$ and $m_J = +1$ atoms [41].
[43] Cayla, H., Carcy, C., Bouton, Q., Chang, R., Carleo, G., Mancini, M. and Clément, D., *Single-atom-resolved probing of lattice gases in momentum space*, Phys. Rev. A **97**, 061609 (2018).
[44] To vary the BEC atom number, we add a magnetic gradient of varying amplitude which increases atom losses during the evaporation in the ODT; this procedure hardly changes the number of impurities because the latter are insensitive to the magnetic gradient. To vary the number of impurities, we hold the BEC and impurities in the ODT for holding times ranging from 0.1 to 3s. The value of the holding time strongly affects the impurity number while it hardly changes the BEC atom number.
[45] We cannot exclude the presence of an algebraic decay the amplitude of which would be too small to be revealed due to the experimental noise.
[46] Lopes, R., Eigen, C., Navon, N., Clément, D., Smith, R. P. and Hadzibabic, Z., *Quantum Depletion of a Homogeneous Bose-Einstein Condensate*, Phys. Rev. Lett. **119**, 190404 (2017).
[47] Tenart, A., Hercé, G., Bureik, J.-P., Dareau, A. and Clément, D., *Observation of pairs of atoms at opposite momenta in an equilibrium interacting Bose gas*, Nature Physics **17**, 1364 (2021).
[48] The data without RF transfer directly yield the tails amplitude $\mathcal{A}_I$ for the impurities only (up to a factor equal to the detection efficiency). To extract $\mathcal{A}_{\rm BEC}$ for the BEC atoms from the measured amplitude $\mathcal{A}$ with RF transfer, we proceed as follows. In the experimental configuration, the RF pulse transfers 34% impurities outside of the detector and 16% BEC atoms onto the detector. Because we have measured $\mathcal{A}_I$ in the absence of RF transfer, we subtract the contribution $0.66 \times \mathcal{A}_I$ from $\mathcal{A}$ and extract the contribution $\mathcal{A}_{\rm BEC}$ from the BEC atoms only: $\mathcal{A}_{\rm BEC} = (\mathcal{A} - 0.66 \times \mathcal{A}_I)/0.16$.
[49] We have also performed additional experiments in slightly different configurations by changing the time-of-flight (from 298 ms to 330 ms) and by applying the RF transfer after a 3 ms time-of-flight (instead of 10 μs). In all those configurations, we observe identical $1/k^4$-tails, which indicates that our observations are immune to these aspects of the experimental procedure.
[50] For the bath-impurity contact $\mathcal{C}^{BI}_{\rm Bogo}$ we also use the LDA, assuming that the dilute impurities do not affect the BEC density profile in the trap. Since the impurities are trapped in a flat-bottom potential and the bath-impurity interaction is weak so that the lowest-order perturbative result holds, we find $\mathcal{C}^{BI}_{\rm Bogo} = (32/5)\pi^2 a^2_{BI} n_{\rm BEC} N_I$.
[51] The latter is indeed equivalent to probing the equation of state at progressively diminishing densities, with the consequence that interaction effects vanish after long expansions.
[52] Astrakharchik, G. E. and Pitaevskii, L. P., *Motion of a heavy impurity through a Bose-Einstein condensate*, Phys. Rev. A **70**, 013608 (2004).
[53] Since we speculate that the algebraic tails may originate from scattering of fast impurities against the BEC, one could wonder if similar tails should appear when thermal atoms scatter against the BEC. However, we do not observe that in our experiment: when the fraction of impurities is negligible, thermal (majority) atoms are certainly present but $1/k^4$-tails are hardly discernable (see Fig. 3). This difference may stem from the fact that thermal (majority) atoms are located on the edge of the trap because they are repelled by the BEC, while the impurities are spread across the BEC as they are trapped in a flat-bottom potential. Fast impurities (above the sound velocity) have therefore a much larger chance to cross the BEC and scatter than the thermal (majority) atoms.